ELSEVIER

Physica D 103 (1997) 590–604

PHYSICA D

Solitary dilation waves in a circular array of liquid columns

F. Giorgiutti *, L. Limat

Laboratoire PMMH, URA CNRS 857, ESPCI, 10 rue Vauquelin, 75231 Paris Cedex 05, France

Abstract

Solitary dilation waves and self-sustained oscillations ("optical" mode) are observed in a one dimensional pattern of liquid columns produced in the pouring of a liquid film from a solid ceiling. A new experiment carried out on a circular fountain allows us to achieve periodic boundary conditions, and thus to observe free propagation of the dilation waves in an infinite medium. Measurements of the drift and group velocities of the dilation waves, and of the "optical" pulsation, are presented as functions of the flow rate. In addition, starting from qualitative observations and order of magnitude estimates, we build a discrete model of non-linear dynamics in this system in which dissipation is compensated by an external energy supply (transient drop formation). This model allows us to recover the appearance of the "optical mode" induced by a wavelength increase and predicts the "focusing" of this mode into a localized "kink" traveling at a constant speed along the column array. The kink structure is reminiscent of the "dilation" waves observed experimentally. Both the model and experiment support a relationship between the wave velocity and the oscillation frequency similar to that observed by Michalland and Rabaud in the "printer's instability".

PACS: 47.20 Ma; 47.54 +r; 46.10 +z; 63.20 Ry

1. Introduction

The observation of localized coherent structures in spatially extended systems is one of the most fascinating discovery of non-linear physics. The initial interest was focused on the "soliton" concept emerging from the study of conservative dynamics [1]. Later, the activity around "pattern forming" instabilities has contributed to open new fields based upon the study of systems with both dispersion and dissipation [2]. In this context, studies of the complex Ginzburg–Landau equation [3] revealed very rich dynamics involving localized structures such as the so-called "pulses", "fronts", "holes", and "spirals" in two dimensions. In another direction, localized objects were also identified in various one-dimensional cellular patterns generated by instabilities, as elementary mechanisms of wave length selection, associated with secondary instabilities of the pattern [4–8]. A typical example is the well known "drift state" observed in solidification front [4,5] and in various hydrodynamic instabilities [6–8], also called "dilation waves" [7] in directional viscous fingering (parity breaking instability). In this case, a local "parity

* Corresponding author.

PII S0167-2789(96)00288-6

breaking" of the pattern (left–right symmetry loss) is accompanied by a drift at a constant speed of the cells, the boundary of the drifting "bubble" propagating also at a constant speed but in a direction opposite to the drift motion.

Very often, this drift state coexists with other dynamical states of the pattern that can be oscillatory. For instance, an "optical" mode in which the position of the cells oscillates, while remaining out of phase with that of its nearest neighbors has been identified in solidification fronts [4,5] and in the "printer's instability" (cellular fingering observed on a liquid meniscus confined between two rotating cylinders) [7]. Usually, the theoretical description of both states (drift and oscillations) involves non-linear equations that couple the spatial phase of the pattern to the real or complex order amplitude associated with the relevant secondary instability of the pattern [11]. The structure of these equations is generally deduced from symmetry arguments, each of the two phenomena being described by its own set of equations with a priori unknown coefficients. This description is most often sufficient but forgets the possible physical relationships between the two phenomena, and remains difficult to extend to situations involving their coexistence and interactions between them.

Recently, Michalland and Rabaud [12] have shown experimentally that, at least for the printer's instability, a physical connection seems to exist between the optical mode and the dilation waves. More precisely, the "group" velocity V_g of the dilation waves (motion of the "bubble") is proportional to the natural velocity built upon the frequency of the optical mode ω_{opt} and upon the pattern wavelength λ observed in the vicinity of both dynamical states:

$$V_g = p\lambda\omega_{opt}, \tag{1}$$

in which p is of order 0.4. They have ascribed this behavior to what they called an "elasticity" of the pattern similar to that of a one-dimensional chain of mass and springs (phonon model). More precisely, if one identifies V_g to the long wavelength approximate of the phonon velocity (sound velocity) and ω_{opt} to the pulsation observed in the boundary of the Brilloin zone (where out of phase stationary oscillations usually occur), one obtains a similar relationship with $p = 0.5$. Rather than a "pattern elasticity" this "phonon model" introduces inertia in the pattern dynamics which can be surprising in a context largely dominated by dissipation. To our knowledge this possible relation between drifting and oscillatory states has never been evidenced in any other pattern, and the generality of Michalland and Rabaud result remains to be proved.

In the present article we reconsider this problem on another pattern, that we studied in two previous papers [8,9], and which we called "the liquid column array" [10]. An example of this pattern is reproduced in Fig. 1. Such a structure consists of parallel liquid columns observed in the pouring of a liquid from a horizontal rectilinear ceiling. This ceiling can be for instance the lower extremity of an inclined plane along which a liquid is flowing, or as in our case in a horizontal cylinder, the liquid flowing from the upper generating line towards the lower one [13]. These columns are not independent from each other as they remain connected by a thin liquid film: our experiments on a cylindrical ceiling [8–10] revealed that the spatial periodicity of this pattern λ, usually of order 10 times the capillary length $l_c = \sqrt{\gamma/\rho g} \simeq 1$ mm (γ surface tension, ρ mass density, g gravity), was in fact perturbed by collective phenomena. When the local wavelength exceeded a given threshold, a secondary oscillatory instability occurred leading to the appearance of a self-sustained optical mode, illustrated by the spatio-temporal diagram inserted in Fig. 1. As usual, this diagram is obtained by recording a line of the picture of the pattern recorded by a video camera at successive times separated by a constant interval. In this state, the position of each column oscillates, its motion and that of its nearest neighbors remaining out of phase. Imposed sinusoidal motions of one boundary column were also investigated in our experiments [9] and revealed a phase diffusion regime at low frequency, progressively replaced by the emission of localized "dilation" waves when the forcing parameters were increased (see Fig. 2).

We present here a new study of these dilation waves carried out in a different geometry [10]: we used a circular overflowing container (a circular "fountain") instead of a horizontal cylinder, in order to realize periodic boundary conditions. In these conditions the propagation can be studied without any perturbations of the boundaries over

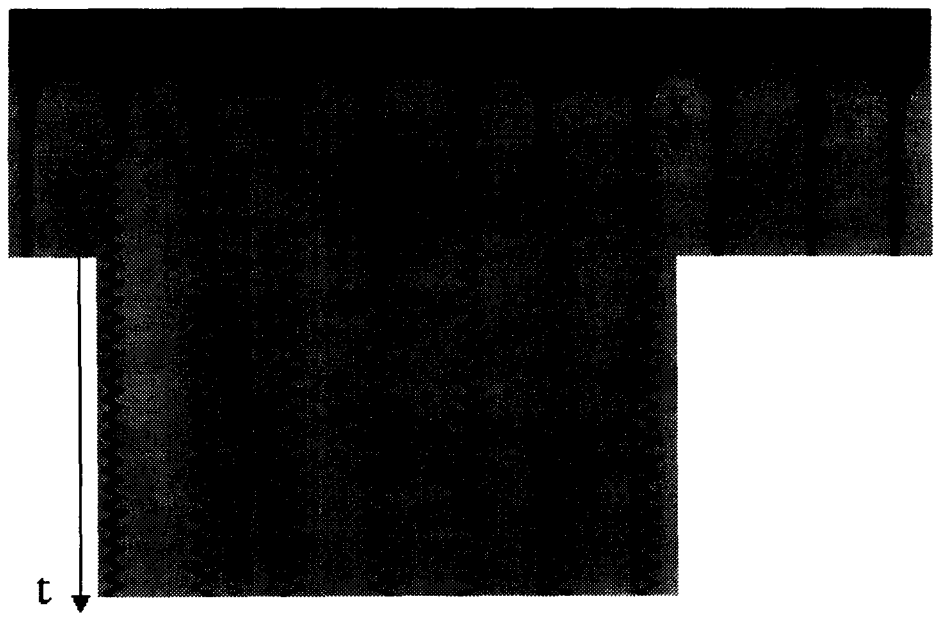

Fig. 1. Liquid column array formed in the pouring of a liquid from an horizontal cylinder (length 28 cm), and typical spatio-temporal diagram giving the horizontal motions of the column as functions of time (running towards the bottom). This diagram is built in the case of an "optical mode" induced by an imposed mean wavelength dilation of the pattern (the position of the boundary columns are imposed by capillary contact with fixed needles).

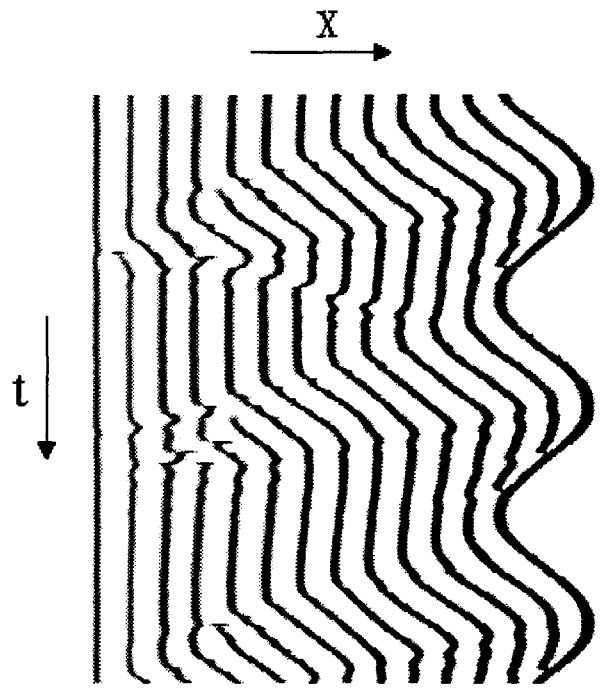

Fig. 2. Spatio-temporal diagram obtained by forcing a sinusoidal motion of a boundary column, in the experiment of Fig. 1. The imposed frequency (0.15 Hz) is 10 times smaller than the "natural" pulsation of the "optical" mode (2 Hz).

very long distances. In addition, starting from the "phonon analogy" [12] and from our qualitative observations in the case of the liquid column array, we try to suggest a new model of the dynamics of a cellular structure that captures both the existence of a "self-sustained" optical mode and that of the dilation waves. Our experimental results are presented in Section 2, in which we investigate the properties of these dilation waves (drift and group velocity) by varying the imposed flow rate. These results are compared to the "natural" velocity $\lambda\omega_{opt}$, the optical pulsation ω_{opt} being measured on localized oscillatory states observed for suitable conditions. As for the printer's instability, a law of the kind $V_g = p\lambda\omega_{opt}$ is obtained with $p \simeq 0.4$. In Section 3, we develop our phenomenological model of the array dynamics: in summary, the array is treated as a one-dimensional chain of mass and springs to which we add a friction term (dissipation), anharmonicity, and additional variables describing the state of the interface connecting two columns. This interface is supposed to undergo a possible localized instability leading to the appearance of a transient drop (experimentally observed), the force exerted by this drop on the liquid column being able to compensate in average the dissipation. Numerical simulations of this model are presented in Section 4, in the case of an array submitted to a uniform wavelength dilation, and placed under periodic boundary conditions. The results are similar to those observed in our experiment: for a suitable choice of the model parameters, a natural state of this system consists of an optical mode that progressively evolves into a solitary kink traveling at constant speed along the column array, the structure of this kink being similar to that of the dilation waves. The speed of this kink is again proportional to the "natural" velocity $\lambda\omega_{opt}$ but with $p = 0.5$ as expected from the initial phonon model.

By nature our model is discrete, which is in contrast with the usual Ginzburg–Landau type approach most often developed at a continuous level [11]. To our knowledge, rather few studies of cellular patterns involved discreteness. Two exceptions are the arrays of vortices forced by magnetic effects in a flowing electrolyte [14], and the arrays of coupled jets in open flows [15]. Although in this paper we do not discuss explicitly the influence of discreteness, specific effects are presumably to be expected in analogy with what happens in the case of conservative dynamics. For instance, in this other field unusual behaviors were identified such as the Peierls–Nabarro barrier encountered by solitons moving on a lattice [16], the unusual breather dynamics in DNA molecules [17], or the spontaneous formation of coherent objects in two-dimensional sine-Gordon lattices [18]. With some respects, cellular structures encountered in diverse instabilities [4–13] can be viewed as equivalents in the "dissipative world" of these discrete materials. We therefore suggest that future studies of our model or of appropriate generalizations of this one could help to understand phenomena occurring on cellular patterns at a very localized scale.

2. Experiment

A picture of our experiment is reproduced in Fig. 3. In comparison, with our previous studies (liquid columns formed below a horizontal cylinder [8,9]), we worked in the same conditions (silicon oil of viscosity 20 cP, same method of flow control), except that the horizontal cylinder was replaced by a plexiglas container of circular perimeter placed at the top of a vertical tube. The container of external radius $R = 5$ cm is supplied with liquid at a constant rate Q (varying in the range 1–10 $cm^3\,s^{-1}$), the liquid rising inside the tube. The liquid fills the container, overflows, runs over its vertical external sides, and falls into the expected spatially periodic array of liquid columns.

The bottom of the container being rigorously flat, we observed that the column center remained distributed on a circle of radius $R' \simeq 4.4$ cm, slightly smaller than R. In these conditions, the most natural state observed was 24 static columns separated by a mean wavelength equal to 1.2 cm. We have tried to perturb the column array as we did in [8,9]: the motion of a column was forced by touching it with a needle, then by moving this needle before removing it in a very short time. Coalescences between columns are forced along the needle trajectory (increase of the mean wavelength) while a few columns following the first one begin to move. After a short transient, a solitary

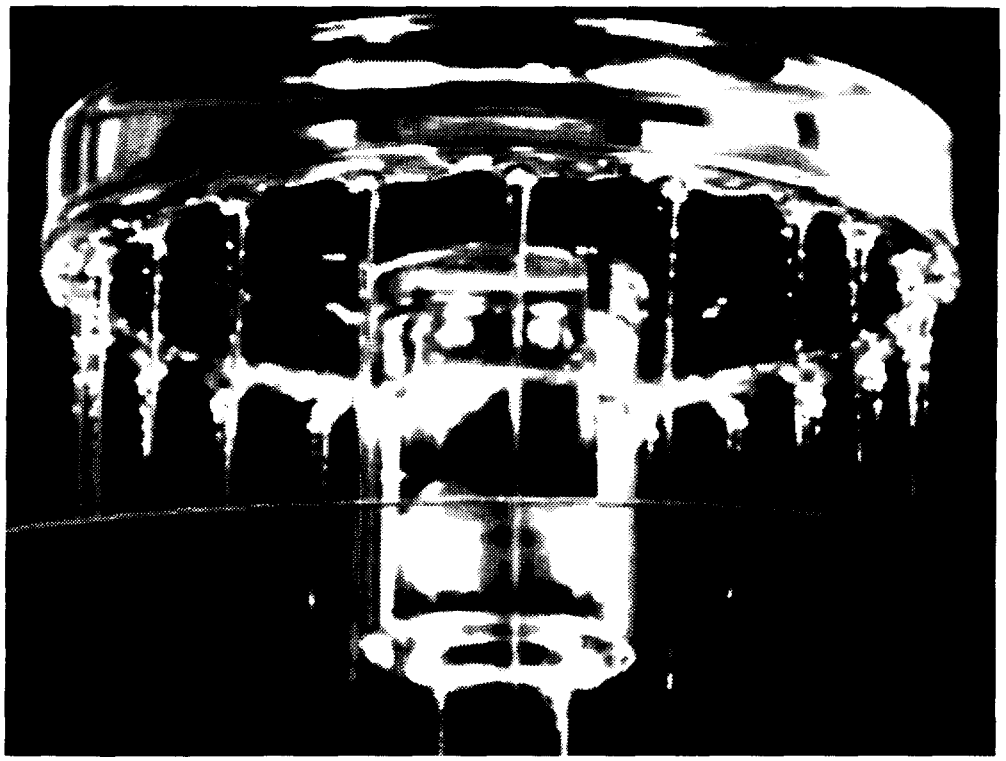

Fig. 3. Picture of the experiment under periodic boundary conditions. The columns are formed in the pouring of a liquid from an overflowing circular container (radius 5 cm) continuously supplied with liquid, the liquid rising inside the central columns supporting the container (circular fountain).

dilation wave was formed and propagate at constant speed along the container perimeter. We followed this motion by building "spatio-temporal" diagrams such as that reproduced in Fig. 4, from video pictures taken from above: owing to the transparency of the container and to the refraction index of the liquid, the column appears as black circles when viewed from above, and gray levels were recorded along a circle cutting all the column centers. We explored the properties of the dilation waves, by varying the flow rate and the launching conditions. We found that different numbers of drifting columns (from one to four in practice) could be forced: as a result, the position jump of the columns introduced after one kink rotation can vary (1 to 4λ) but the group velocity V_g of the wave (motion of the wave boundaries) as well as the individual drift velocity V_d of the columns were the same in all cases. A few measurements of these velocities are plotted in Fig. 5(a) as functions of the flow rate. Both velocities are of order of a few centimeter per second. The group velocity V_g increases with the flow rate, while the drift velocity V_d slightly decreases.

The pulsation of the optical mode ω_{opt} was measured in separate experiments by slightly tilting the container. This inclination induces a weak gravity component parallel to the cylinder perimeter that slightly increases the wavelength in the upper region of the container. When this local wavelength dilation exceeded the optical threshold, the optical mode appeared and its frequency was measured using again spatio-temporal diagrams. These measurements are displayed in Fig. 5(a). Just like the group velocity of the dilation waves, the optical frequency ν_{opt} increases with the flow rate. We have tried to establish a connection between both variations by comparing the group velocity V_g to the natural velocity $V_0 = V_g/\lambda\omega_{opt}$ built upon the wavelength λ left outside of the dilation waves (nearly constant and

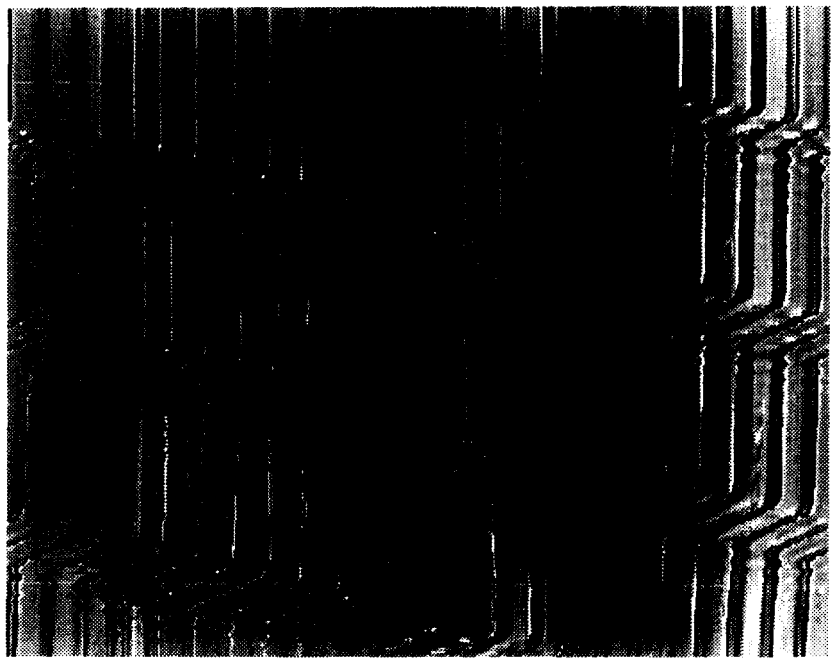

Fig. 4. Spatio-temporal diagram obtained from video pictures recorded from above, across the circular container. Time runs toward the bottom, the horizontal axis being the angular position of the columns. At the beginning of the experiment, a column motion is forced by a sudden motion of a needle in contact with the top of a column.

equal to 1.1 cm), and upon the optical pulsation $\omega_{opt} = 2\pi \nu_{opt}$. The result of this comparison appears in Fig. 5(b). Our measurements (performed in the range 5–10 $cm^3\ s^{-1}$) suggest that the ratio V_g / V_0 remains constant and equal to 0.4 ± 0.05 in agreement with Eq. (1). The slope value ($p = 0.4$) is close to that obtained by Michalland and Rabaud for the printer's instability. Their result seems therefore to possess a high degree of generality, as was to be expected in view of the simplicity and generality of the phonon analogy.

3. Model

3.1. General ideas

Visualizations of the column motions are presented in Figs. 6(a) and (b), respectively in the case of the optical mode and in that of the propagating dilation waves. The basic idea of our model consists in treating each column "meniscus" (top of a column), of index i, as a moving object described by its horizontal position $X_i(t)$. Each meniscus i is supposed to interact with its nearest neighbors of indices $i + 1$ and $i - 1$ by an harmonic potential possibly completed by anharmonicity terms, and also with transient drops formed between each pair of neighbors. These transient drops are visible in Figs. 6(a) and (b). In the case of the optical mode, the structure of this drop is symmetrical with respect to the center of the two neighboring columns, this symmetry being lost in the case of the dilation waves. We, therefore conjectured that the description of the drop dynamics required at least two independent variables (see Fig. 7) Y_i and Z_i. Intuitively, the first variable Y_i measures the drop height or equivalently the total amount of liquid contained in the drop, while the second one Z_i measures the degree of asymmetry of the liquid

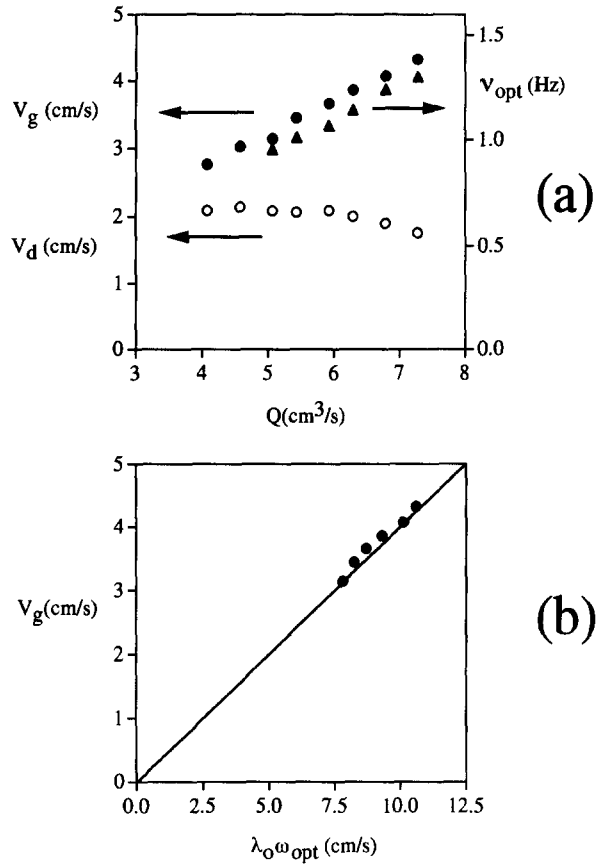

Fig. 5. (a) Measurements of the group velocity V_g and of the drift velocity V_d of the dilation waves for different values of the total flow rate Q, in the experiment of Fig. 3. Measurements of the frequency of the "optical mode" ν_{opt} are also displayed. (b) Comparison of the group velocity V_g to the "natural" velocity $V_0 = \lambda\omega_{opt}$ built on the "optical" pulsation $\omega_{opt} = \nu_{opt}$ and on the wavelength λ left behind the dilation wave. The slope of the solid line is equal to 0.4.

mass distribution. A simple interpretation of these two quantities is given in Fig. 7, based on a two-point description of the interface connecting two liquid columns: one may decide that a quantity $Y_i - Z_i$ of liquid is located near the column $i-1$, while the amount $Y_i + Z_i$ is located near the other column $i+1$. In the following sections we present the details of our model and try to justify some of the approximations by a few order of magnitude estimates.

3.2. Column dynamics

One has to suggest plausible equations governing the column motion and its coupling with the drop coordinates. The simplest idea consists in completing the phonon model by a friction term, and by possible anharmonicity effects:

$$m\frac{d^2X_i}{dt^2} + f\frac{dX_i}{dt} = K(X_{i+1} - 2X_i + X_{i-1}) + K\delta[(X_{i+1} - Xi)^3 + (X_{i-1} - X_i)^3] + F_i \qquad (2)$$

in which m is an effective mass that will be estimated later, f is a phenomenological friction coefficient and F_i are the forces exerted on the columns by the transient drops. The physical origin of the harmonic interaction described

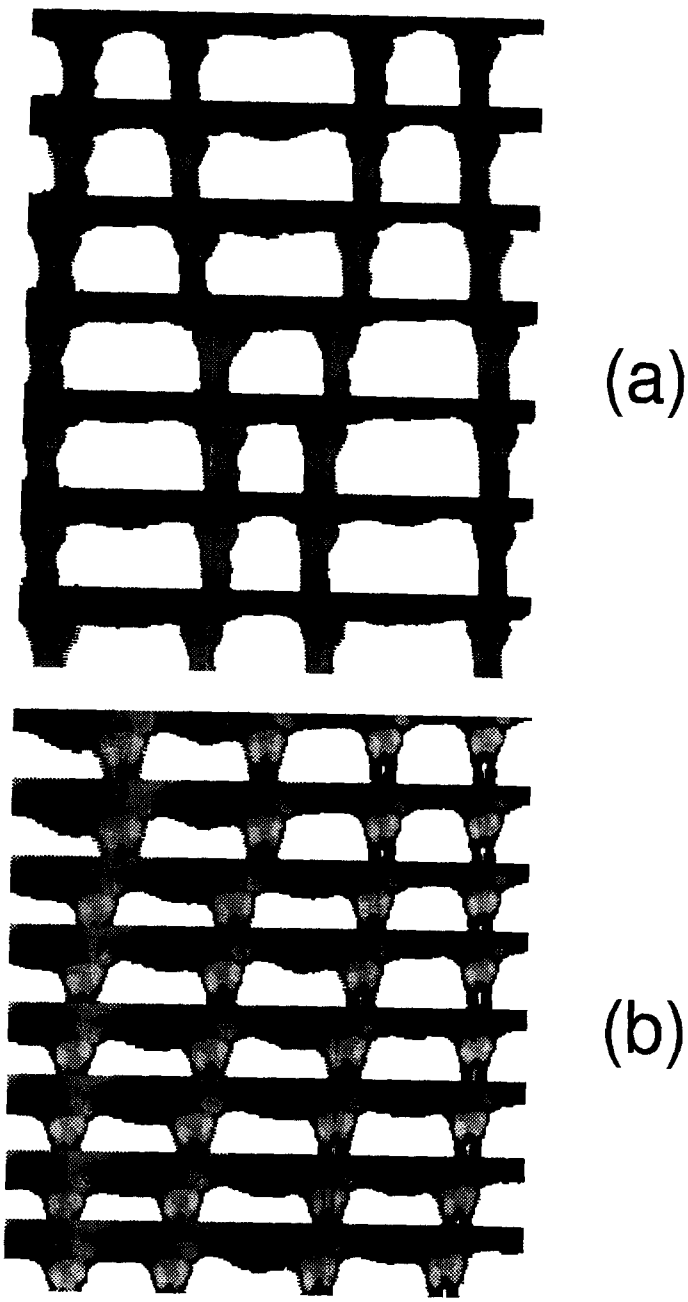

Fig. 6. (a) Successive snapshots of the column motion in the case of the optical mode. Only the top of the columns and the free surface of the film hanging below the horizontal cylinder of Fig. 1 are made visible. The column motion is coupled with the appearance of transient pendant drops. (b) Drifting columns in the case of a "dilation" wave.

by the rigidity constant K is not obvious but is presumably related to surface tension effects. This can be made more quantitative by estimating the typical pulsation ω_0 defined as $\omega_0^2 = K/m$. Fig. 6 suggests a typical mass of order $m \simeq 8\pi\rho l_e^3$, l_e being a typical size close to the capillary length l_c (0.1 cm in [8–10]). Dimensionally, one can hope that K is of order of the surface tension $\gamma \simeq 20\ \mathrm{dyn\,cm^{-1}}$. With $\rho \simeq 1\ \mathrm{g\,cm^{-3}}$, one gets $\omega_0 \simeq 30\ \mathrm{s^{-1}}$ which

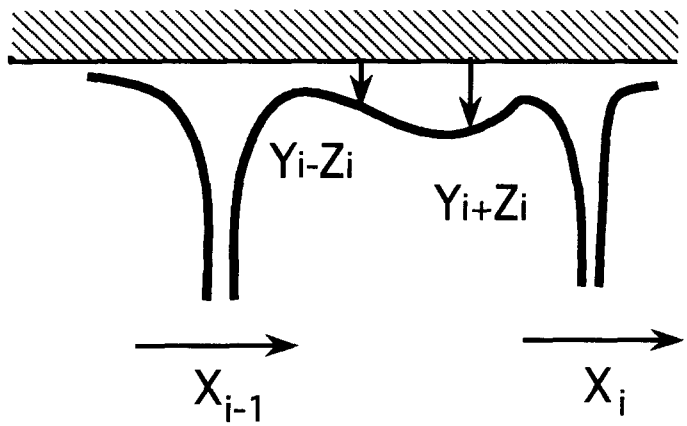

Fig. 7. Notations and geometry involved in the model. The displacement X_i of a column (i) is coupled with that of its nearest neighbors and with variables describing a possible transient drop formation (instability of the interface connecting two columns): Y_i drop amplitude, Z_i drop asymmetry.

is a bit large but remains comparable to the data obtained in [8], $\omega_{opt} \simeq 12\,s^{-1}$. Concerning the anharmonicity, the selected form is arbitrary but other choices did not seem to modify appreciably the obtained results.

The most important feature of our model is the coexistence of an inertia term and of a dissipative one in the left-hand member of Eq. (2). The presence of a first-order time derivative (friction term) ensures us to recover at low frequency the classical phase diffusion behavior explored in [9,10], while the second-order one should allow us to recover the "phonon properties" invoked by Michalland and Rabaud [12]. The coexistence of both terms (inertia and friction) can also be justified with a few orders of magnitude: the dissipation constant f includes the effects of viscosity and of the momentum flux communicated to the liquid ejected in the column. The first contribution to f should be of order $f_1 \simeq \pi \eta l_e$, the second contribution being equal to the mass flux per column $f_2 = q$ ($q \simeq 0.2\,g\,s^{-1}$ in [8]). Using the mass estimate discussed above, and available data [8] relative to the optical mode (amplitude $A \simeq 0.1\,cm$, pulsation $\omega \simeq 6\,s^{-1}$) and to the liquid properties ($\rho \simeq 1\,g\,cm^{-3}$, $\eta = 20$ cP) give typical ratios between inertia and the two dissipative terms of order $mA\omega^2/f_1 A\omega \simeq \rho\omega l_c^2/\eta \simeq 2$ and $f_1/f_2 \simeq q/(\pi l_c \eta) \simeq 3$. This confirms that both inertia and dissipation had to be included in the model.

3.3. Drop–column interaction

The dissipation term added to the phonon model in the previous part allows us to recover the phase diffusion behavior at low frequency but should obviously lead to a damping of the column oscillations. One, therefore, needs an "external" source of energy that should be contained in the drop–column interaction. Previous investigations of the behavior of ordered lattices of pendant drop [19] have revealed that two overlapping pendant drops-exhibit a pronounced tendancy to coalesce. In analogy with this simple observation we have conjectured that the drop–column interaction was attractive. For simplicity, we have also assumed that the drop–column interaction was a linear function of the drop amplitude Y_i and of the drop asymmetry Z_i. This is of course somewhat arbitrary but constitutes the simplest available choice:

$$F_i = A_1[Y_{i+1} - Y_i] - A_2[Z_i + Z_{i+1}] \tag{3}$$

in which A_1 and A_2 are two positive constants. The sign choices are made in order that the drops (i) and $(i+1)$ exert antagonist attractive forces on column (i), and also in order that an asymmetric drop exerts a larger force on

the nearest of its two neighboring columns. This expression can also be justified in the case $A_1 = A_2$ by assuming that the force exerted on the right-hand side of the column i is proportional to $Y_{i+1} - Z_{i+1}$, while the left hand one is proportional to $Y_i + Z_i$. With some respect, the Z-component of the force plays the role of the parity breaking terms governing the spatial phase drift in the theory developed by Coullet, and Gunaratne and coworkers [11].

3.4. Drop dynamics

In the description of the drop dynamics, we assumed that the drop formation was in fact the result of an instability of the interface connecting two neighboring columns. We, therefore, retained a Landau type equation for the growth equation of Y_i, in which the local distance $X_i - X_{i-1}$ between columns plays the role of a control parameter:

$$(1/\sigma)\frac{dY_i}{dt} = [X_i - X_{i-1} - \epsilon_c - q_3 Z_i^2]Y_i + \beta_1 Y_i^2 - \beta_2 Y_i^3. \tag{4}$$

In this equation, ϵ_c designates the threshold of drop formation, σ the typical growth rate of the drop, β_1 and β_2 are numerical coefficients. We assumed β_1 possibly non-zero because $+Y_i$ and $-Y_i$ are presumably not equivalent. In addition, we introduced a damping term $q_3 Z_i^2 Y_i$, because some of our observations revealed a systematic disappearance of the transient drops when they approach one of the two neighboring columns.

The last equation that governs the drop asymmetry is certainly the most difficult to build. Following a rule of maximum simplicity we have postulated the following equation:

$$(1/\sigma)\frac{dZ_i}{dt} = -q_1 Z_i - q_2 Y_i \left[\frac{dX_i}{dt} + \frac{dX_{i-1}}{dt}\right]. \tag{5}$$

In this equation, the origin of the drop asymmetry is attributed to the mean motion of the columns, the drop being supposed to appear with a zero horizontal velocity: we admit that the amount of liquid shift from the center of the two columns is presumably proportional to the whole mass of liquid available (that is to Y_i) and to the mean velocity of the columns. The strength of this effect is measured by another constant q_2. We have also introduced a restoring constant q_1, because intuitively, the uniformity of the flow supply should tend to favor $Z_i = 0$.

3.5. Reduced equations – Choice of the parameters

After defining an eigen pulsation as $\omega_0^2 = K/m$, a reduced friction coefficient $f_r = f/m$, and two reduced drop column interaction coefficients $\alpha_1 = A_1/m$ and $\alpha_2 = A_2/m$, the whole set of equations defining our model can be put under the form:

$$\frac{d^2X_i}{dt^2} + f_r\frac{dX_i}{dt} = \omega_0^2(X_{i+1} - 2X_i + X_{i-1}) + \omega_0^2\delta[(X_{i+1} - Xi)^3 + (X_{i-1} - X_i)^3] - \alpha_1[Y_{i+1} - Y_i] + \alpha_2[Z_i + Z_{i+1}], \tag{6a}$$

$$(1/\sigma)\frac{dY_i}{dt} = [X_i - X_{i-1} - \epsilon_c - q_3 Z_i^2]Y_i + \beta_1 Y_i^2 - \beta_2 Y_i^3, \tag{6b}$$

$$(1/\sigma)\frac{dZ_i}{dt} = -q_1 Z_i - q_2 Y_i \left[\frac{dX_i}{dt} + \frac{dX_{i-1}}{dt}\right]. \tag{6c}$$

Its structure is somewhat arbitrary but, as we shall see, leads to interesting behaviors very similar to those observed experimentally. Strictly speaking it must not be taken as a rigorous model of the liquid column array, but rather as

a first and rough attempt of such a model. One can also consider this model as a simple dynamical system that is expected to share a lot of properties with the liquid column array and possibly with other cellular structures. Our physical expectation is that the essential features are in fact contained in the first equation (competition between inertia and dissipation), and in the general idea of a two-variable description of the transient drop dynamics. The choices made in the modeling of these drop dynamics are supposed to be of comparatively less influence on the general properties of the dynamics of this system.

The behavior of our model has been explored by means of numerical simulations described in Section 4. The choice of the numerical values of the parameters is not obvious: some of them are constrained by the available experimental data, while others would require specific measurements not yet available. In the numerical simulations, we have reduced the number of free parameters as follows. We first retain the eigen pulsation ω_0 as a "natural" time unit, i.e. we assumed for simplicity $\omega_0 = 1$. Two other time constants must be specified now: the friction coefficient f_r and the time constant σ entering the drop dynamics equations. The first one is in fact specified by our previous measurements [9,10] of the optical pulsation and of the phase diffusion coefficient D that describes the diffusive, low frequency limit of the pattern dynamics governed by a diffusion equation [20]. The correspondence between this equation written at a continuous level and the linear part of our discrete model implies the relationship $f_r/\omega_0 = a^2\omega_0/D$. On the other hand, the phonon analogy discussed by Rabaud and Michalland [12] implies that the optical pulsation is given by $\omega_{opt} = 2\omega_0$, and thus the ratio f_r/ω_0 retained in our model must be equal to $f_r/\omega_0 = a^2\omega_{opt}/2D$. Our previous measurements [8] lead to values of order $\omega_{opt} \simeq 6\,\text{Hz}$ and $D \simeq 20\,\text{cm}^2\,\text{s}^{-1}$ and so to $f_r/\omega_0 \simeq 0.3$. We therefore retained the value $f_r = 0.3$ (together with $\omega_0 = 1$) in the numerical simulations of the model.

Concerning the other time constant σ, repeated simulations convinced us that self-sustained dynamics (i.e. without damping) required large values of this parameter compared to the natural pulsation ω_0 of the columns. This means that, qualitatively, the compensation of the mean dissipation requires a fast enough growth of the transient drops. In practice, a moderate value ($\sigma = 10$) was found to be sufficient while avoiding problems with the time resolution of the numerical code.

4. Numerical simulations

Using a fourth-order Runge–Kutta algorithm, 20 columns ($i = 1$ to $N = 20$) submitted to a uniform wave length dilation $\epsilon = \delta\lambda/\lambda$ were then simulated. Periodic boundary conditions were achieved by shifting of a constant amount the position of two fictive boundary columns ($i = 0$ and $i = N + 1$) from the "true" value expected at the other boundary. At $t = 0$, the initial distributions of X_i, Y_i and Z_i were slightly perturbed by a random noise of typical amplitude 10^{-2}. A typical evolution of the column positions X_i and of the drop variables Y_i and Z_i is depicted in Figs. 8(a)–(c). One observes a progressive growth of the optical mode with an irregular amplitude distribution. Later, a "focusing" of the perturbation occurs leading to a propagating "kink" traveling at a constant speed along the column array.

We tried different values of the remaining free parameters, while remaining as close as possible to values of order unity. Among diverse possibilities, the values $\alpha_1 = 1.5$, $\alpha_2 = 1.0$, $\beta_1 = -0.5$, $\beta_2 = 0.5$, $q_1 = 1.0$, $q_2 = 0.5$ were found to give interesting behaviors. We used various values of the last parameters: δ (anharmonicity), applied wavelength dilation $\epsilon = (X_{N+1} - X_1)/N$ ($N = 20$ column number), and ϵ_c (drop formation threshold for the inter-column distance with respect to a reference state). The kink "stability" was not always satisfied (damping effects) and required a large enough value of the "anharmonicity" factor δ combined with a large enough effective wavelength dilation $\epsilon - \epsilon_c$. On the other hand, shock formation was observed for low and moderate values of the damping constant q_3 of the drop amplitude associated to the asymmetry parameter. Finally, the

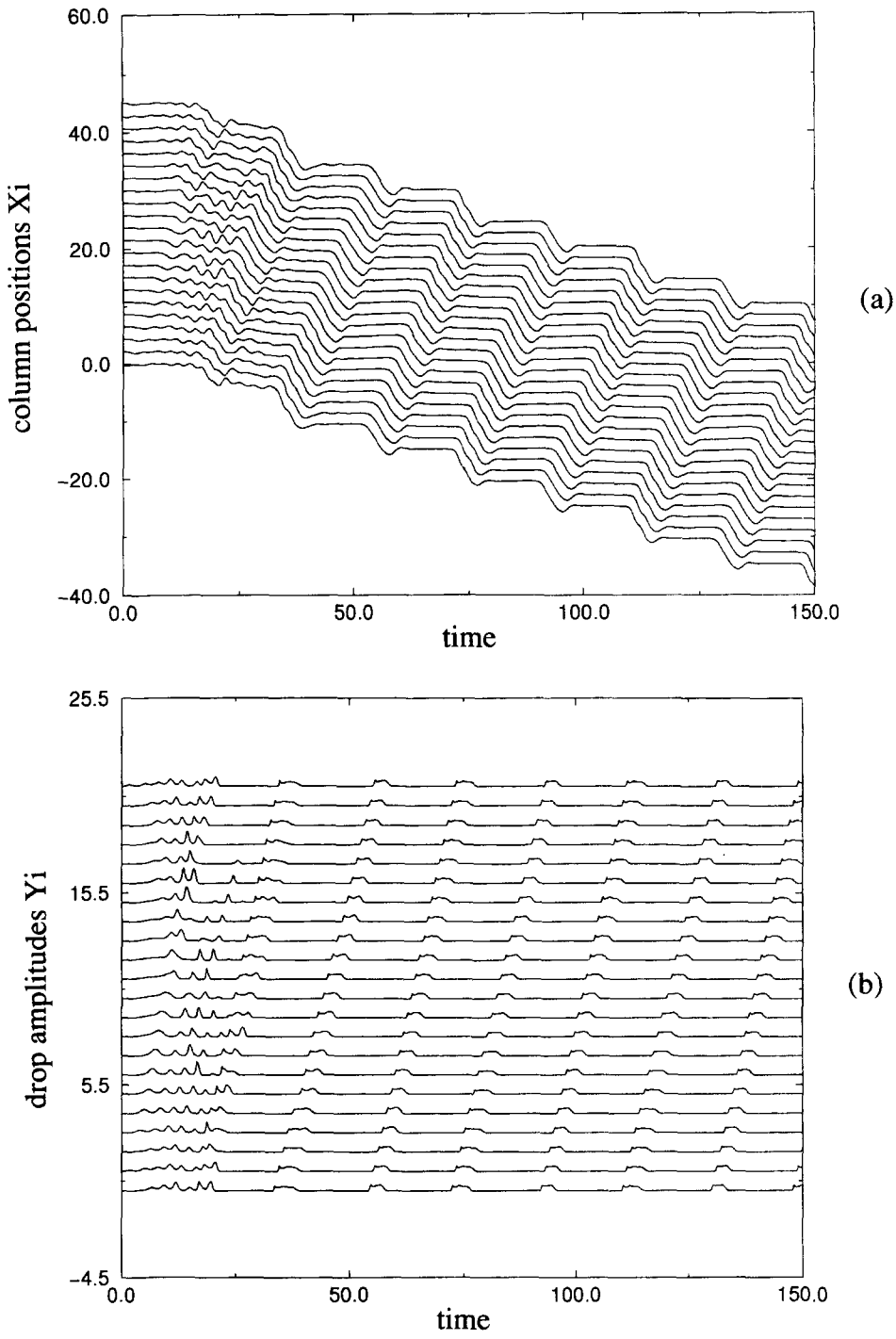

Fig. 8. (a) Evolution of the positions $X_i(t)$ of $N = 20$ columns simulated under periodic boundary conditions. The parameter of the simulations are $\alpha_1 = 1.5$, $\alpha_2 = 1.0$, $f/m = 0.3$, $\omega_o^2 = 1.0$, $\delta = 0.3$,$\sigma = 5.0$, $\beta_1 = -0.5$, $\beta_2 = 0.5$, $q_1 = 1.0$, $q_2 = 0.5$, $q_3 = 10$, $\epsilon_c = 0.015$. The applied strain is constant and equal to $(X_N - X_o)/(N\lambda) = 0.15$. (b) Drop amplitude evolution $Y_i(t)$. (c) Drop asymmetry evolution $-Z_i(t)$. All the curves are shifted for clarity.

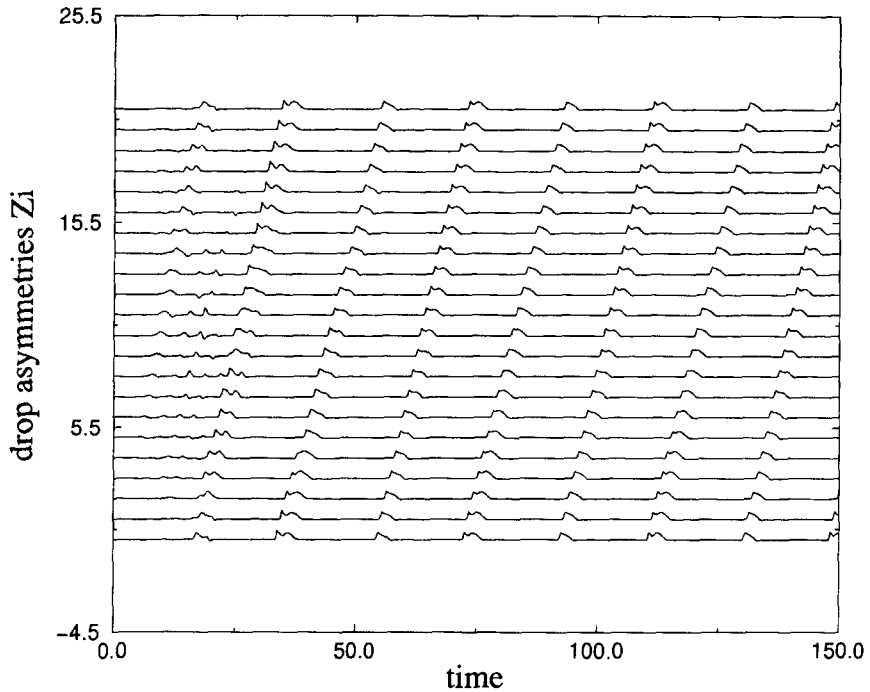

Fig. 8. Continued.

simulations of Fig. 8 were obtained with the values $q_3 = 10$, $\delta = 0.6$, $\epsilon_c = 0.015$, and $\epsilon = 0.15$. Other choices were of course possible, but the range of stability (no damping and no shock formation) seemed to be rather narrow.

In a second step, we have tried to vary the eigen pulsation ω_0 while keeping constant the other parameters. We have then measured the observed optical frequency ω_{opt}, and the group velocity V_g of the dilation waves in order to test again Michalland and Rabaud relationship. The stability of the kink was not always satisfied, and in addition, slight modulations of its properties over long time scales were observed which have limited the accuracy and the number of our measurements. The optical pulsation was also difficult to measure with accuracy because of the irregularity of the optical mode that can be noticed in Fig. 8. In all the stable cases the velocity of the kink V_g was found to be slightly larger (of a factor of order 5%) than the phonon group velocity $V_o = \lambda\omega_o$ built upon the eigen pulsation ω_o and upon the lattice spacing λ (arbitrary shift between the X_i curves in Fig. 2(a)). This fact is reminiscent of Michalland and Rabaud [10] analysis of the phonon model, except that in our case, the dilation waves are non-dispersive and seem to propagate with nearly a constant shape. In addition, they propagate freely although the system is dissipative, presumably because of the external energy supply associated with the transient drop formation. Concerning the optical pulsation, we found values of order $\omega_{opt} \simeq 2.1\omega_o$, while $V_g \simeq 1.05\lambda\omega_o$, which implies a relationship between both quantities given by

$$V_g \simeq 0.5\lambda\omega_{opt}, \tag{7}$$

that coincides with the phonon analogy. This result is suggested in Fig. 9 in which we have plotted our numerical determinations of V_g as functions of the natural velocity $\lambda\omega_{opt}$. Therefore, it seems that the relationship $V_g = p\lambda\omega_{opt}$ is still valid in the case of our non-linear, dissipative model, with $p = 0.5$ just as for the initial phonon model.

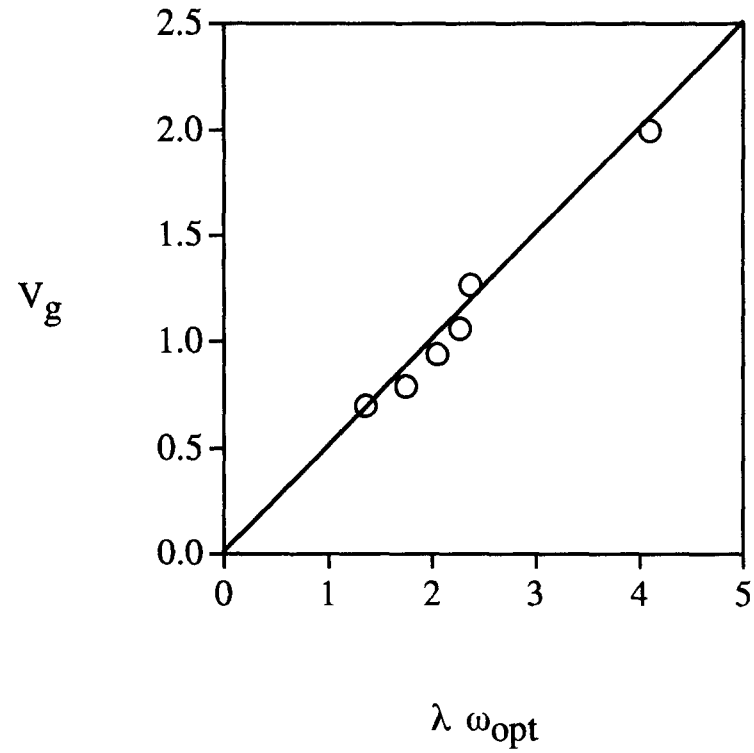

Fig. 9. Comparison between the numerical estimates of the group velocity V_g and the natural velocity $\lambda\omega_{opt}$ built on the pulsation of the optical mode. All the parameters are identical to those of Fig. 8 except the eigen pulsation ω_0 that was variable. The slope of the solid line is equal to 0.5.

5. Conclusion

In summary we have built a phenomenological, discrete, model of the liquid column array. In contrast with the usual description based on continuous equations of Ginzburg–Landau type combined with a phase diffusion equation [11], our model is a discrete one. In addition, it contains both the possibility of an "optical" mode and that of the "dilation" waves, together with the diffusive properties (not simulated here) usually observed at low frequency. This is in fact its main interest, because the Ginzburg–Landau type approach usually looses the coexistence of the three phenomena. We have presented numerical simulations of this model and compared the results with "real" experiments, both studies being carried out in the case of periodic boundary conditions. The model allowed us to recover the existence of a self-sustained optical mode and predicts the focusing of this mode into a "solitary kink" of structure similar to that of the "dilation waves" encountered in other one-dimensional cellular structures. We were able to observe this "kink" in an experiment that reproduces these periodic boundary conditions. Just as for the the printer's instability, its velocity is proportional to the "natural" velocity built upon the pulsation of the "optical mode" and upon the wavelength of the pattern left outside of the dilation wave. In the numerical simulations of our model, the prefactor of this law is equal to the value deduced from the phonon approximation developed by Michalland and Rabaud [12]. In our experimental case, the prefactor is smaller and its value is close to that obtained for the printer's instability ($V \simeq 0.4\lambda\omega_{opt}$ instead of $0.5\lambda\omega_{opt}$). More accurate measurements of the proportionality factor, combined with more extensive simulations of our model are under way. Other behaviors than those discussed in the present

paper can be observed numerically and will be developed in a future publication: chaotic oscillations, localization tendencies of the optical mode, dilation waves generated by a moving boundary, diffusion at low frequency, etc.

We suggest that similar models could be built for other patterns and could allow one to recover specific behaviors not reducible to large scale continuous amplitude equations [2,11]. In addition, as our model mixes inertia and dissipation it could perhaps provide a possible "bridge" between conservative and unconservative non-linear dynamics in discrete systems.

Acknowledgements

We are indebted to O. Cardoso and H. Willaime for advice in image processing, and to H. Herrmann, A. Kulago, J. Lega, A.C. Newell, J.F. Paquerot, H. Stone and J.E. Wesfreid for valuable discussions. We thank O. Brouard, P. Jenffer, G. Marteau and D. Vallet for technical assistance. We acknowledge the support from the Centre National d'Etudes Spatiales (CNES, France).

References

[1] A.C. Newell, Solitons in mathematics and physics (SIAM, Philadelphia, PA, 1986); P.G. Drazin and R.S. Johnson, Solitons: An Introduction (Cambridge University Press, Cambridge, 1989); M. Remoissenet, Waves called Solitons: Experiments and Theoretical Concepts (Springer, Berlin, 1994).
[2] J.E. Wesfreid, H. Brand and P. Manneville, Propagation in Systems far from Equilibrium (Springer, Berlin, 1988); A.C. Newell, T. Passot and J. Lega, Ann. Rev. Fluid Mech. 25 (1993) 399; P.C. Hohenberg and M. Cross, Rev. Modern Phys. 65 (1993) 851.
[3] S. Fauve and O. Thual, Phys. Rev. Lett. 64 (1990) 282; S. Popp, O. Stiller, I. Aranson, A. Weber and L. Kramer, Phys. Rev. Lett. 70 (1993) 3880.
[4] J.-M. Flesselles, A.J. Simon and A.J. Libchaber, Adv. Phys. 40 (1991) 1.
[5] G. Faivre and S. Mergy, Phys. Rev. A (1992).
[6] F. Daviaud, M. Dubois and P. Berge, Europhys. Lett. 9 (1989) 441; I. Mutabazi, J.J. Hegseth, C.D. Andereck and J.E. Wesfreid, Phys. Rev. Lett. 64 (1990) 1729.
[7] M. Rabaud, S. Michalland and Y. Couder, Phys. Rev. Lett. 64 (1990) 184; H.Z. Cummins, L. Fourtune and M. Rabaud, Phys. Rev. E 47 (1993) 1727; L. Pan and J.R. de Bruyn, Phys. Rev. E 49 (1994) 483.
[8] L. Limat, P. Jenffer, B. Dagens, E. Touron, M. Fermigier and J.E. Wesfreid, Physica D 61 (1992) 166.
[9] F. Giorgiutti, A. Bleton, L. Limat and J.E. Wesfreid, Phys. Rev. Lett. 74 (1994) 538.
[10] F. Giorgiutti, Dynamics of a liquid column array, Thesis, Univ. Paris 6 (1995).
[11] R.E. Goldstein, G.H. Gunaratne, L. Gil and P. Coullet, Phys. Rev. A 43 (1991) 6700; P. Coullet and G. Iooss, Phys. Rev. Lett. 64 (1990) 866; F. Daviaud, J. Lega, P. Berge, P. Coullet and M. Dubois, Physica D 55 (1992) 287; A different approach is based on an interaction between the base mode and its first harmonic: see e.g. S. Fauve, S. Douady and O. Thual, J. Phys. II (France) 1 (1991) 311.
[12] S. Michalland and M. Rabaud, Physica D 61 (1992) 197.
[13] W.G. Pritchard, J. Fluid Mech. 165 (1986) 1; G.M. Carlomagno, Proc. 2nd AIMETA Congr. (Napoli, Italie, October 1974); L. de Luca and C. Meola, J. Fluid Mech. 300 (1995) 71.
[14] H. Willaime, O. Cardoso and P. Tabeling, Phys. Rev. Lett. 67 (1991) 3247.
[15] M.P. Chauve and P. Le Gal, Physica D 58 (1992) 407–413; E. Villermaux and E.J. Hopfinger, J. Fluid Mech. 263 (1994) 63–92; E. Villermaux and E.J. Hopfinger, Physica D 72 (1994) 230–243; M. Fullana, P. Le Gal , M. Rossi and S. Zaleski, Physica D, submitted.
[16] Y.S. Kivshar and D.K. Campbell, Phys. Rev. E 48 (1993) 3077.
[17] T. Dauxois, M. Peyrard and C. Willis, Physica D 57 (1992) 267.
[18] J.M. Tamga, M. Remoissenet and J. Pouget, Phys. Rev. Lett. 75 (1995) 357; ibid (1995) 4156.
[19] M. Fermigier, L. Limat, J.E. Wesfreid, P. Boudinet and C. Quilliet, J. Fluid Mech. 236 (1992) 349.
[20] P. Manneville, Dissipative Structures and Week Turbulence (Academic Press, New York, 1990).